

FIG.1(A)(1)

FIG.1(A)(2)

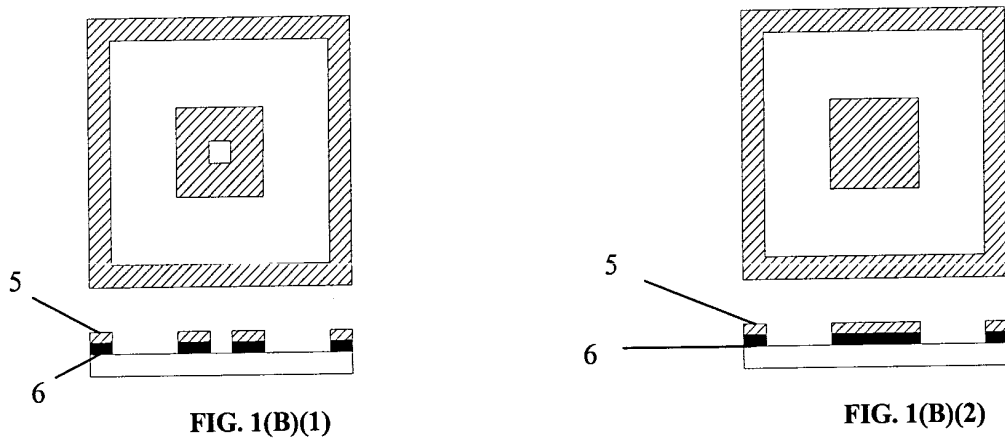


FIG. 1(B)(1)

FIG. 1(B)(2)

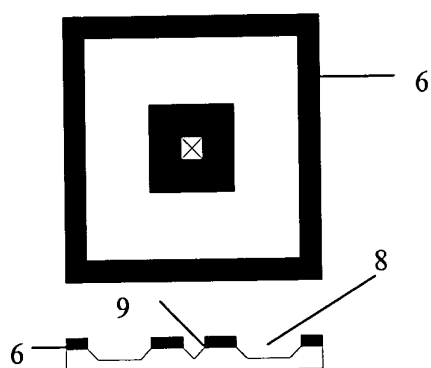


FIG. 1(C)(1)

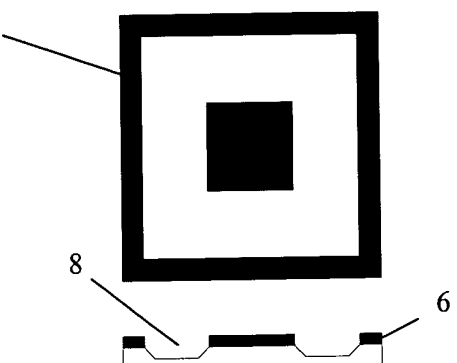


FIG. 1(C)(2)

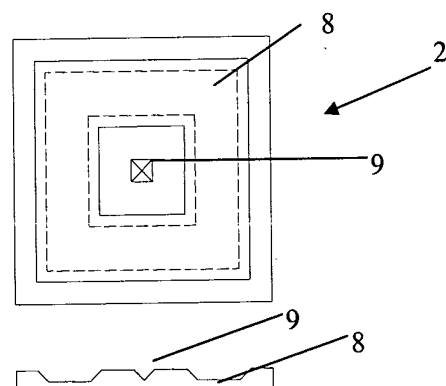


FIG. 1(D)(1)

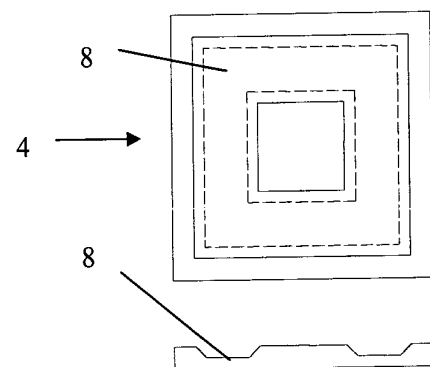


FIG. 1(D)(2)

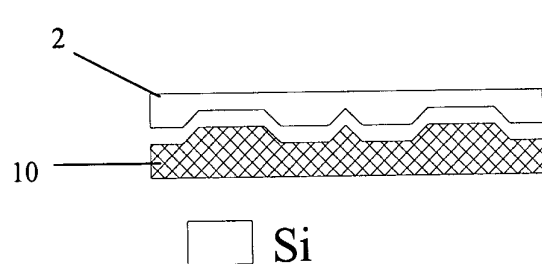


FIG. 1(E)(1)

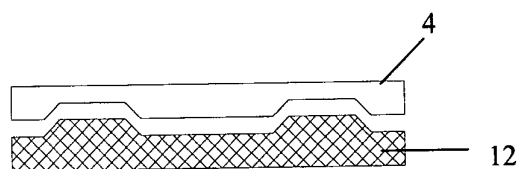


FIG. 1(E)(2)

 Metal

 PMMA

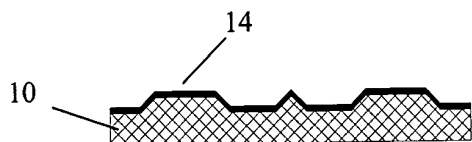


FIG. 1(F)(1)

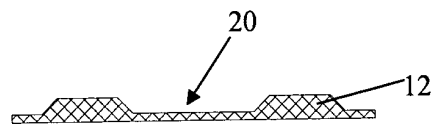


FIG. 1(F)(2)

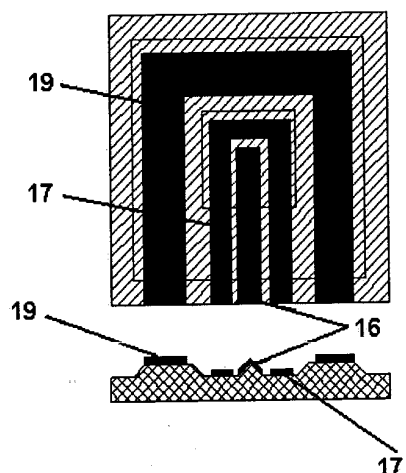


FIG. 1(G)(1)

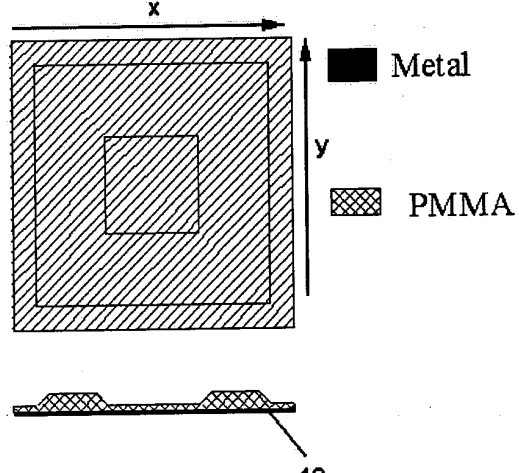


FIG. 1(G)(2)

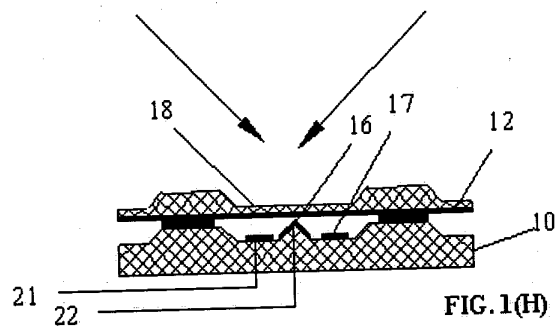


FIG. 1(H)

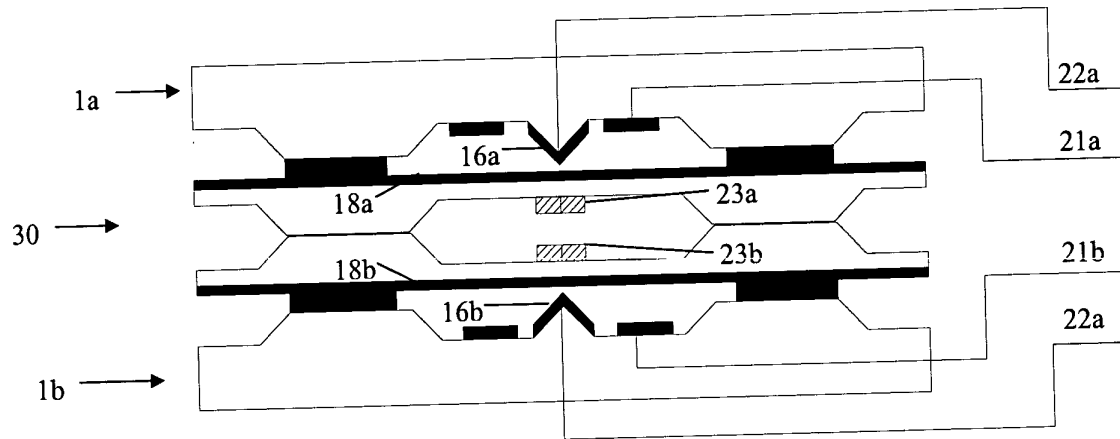


FIG. 2(A)

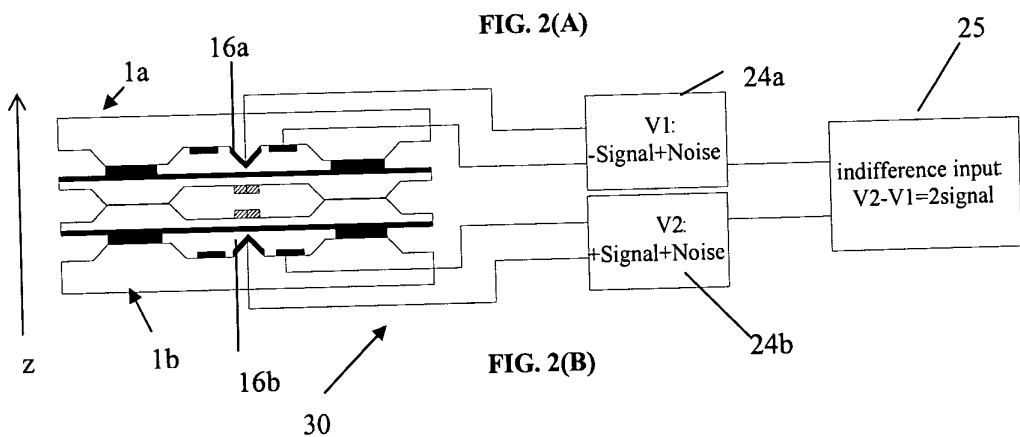


FIG. 2(B)

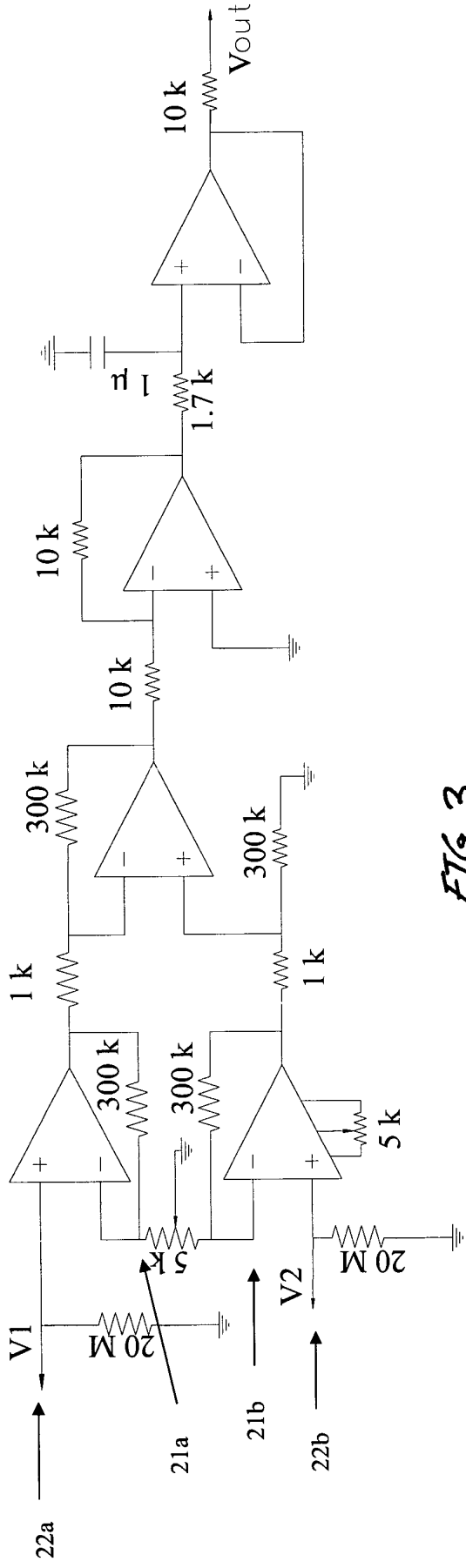
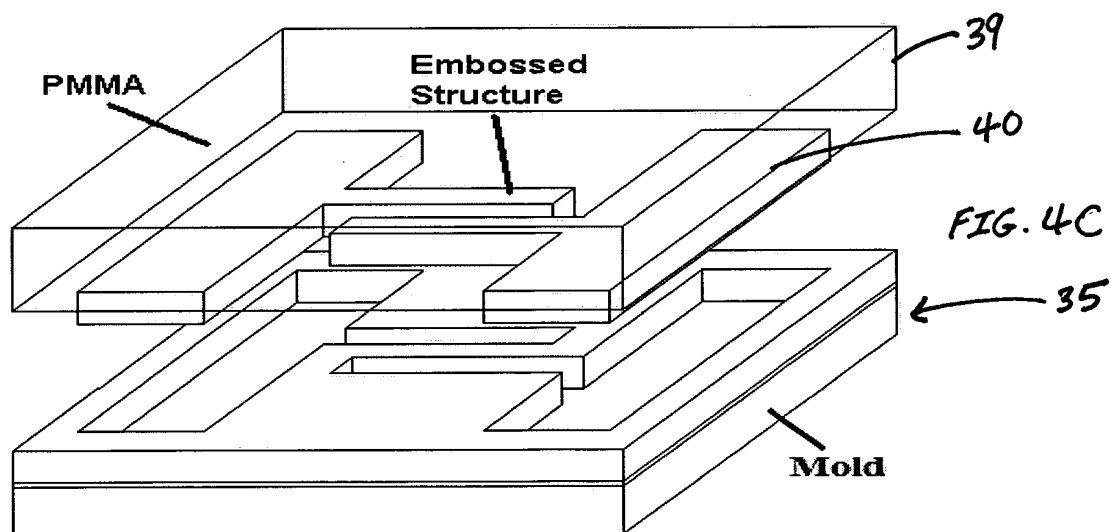
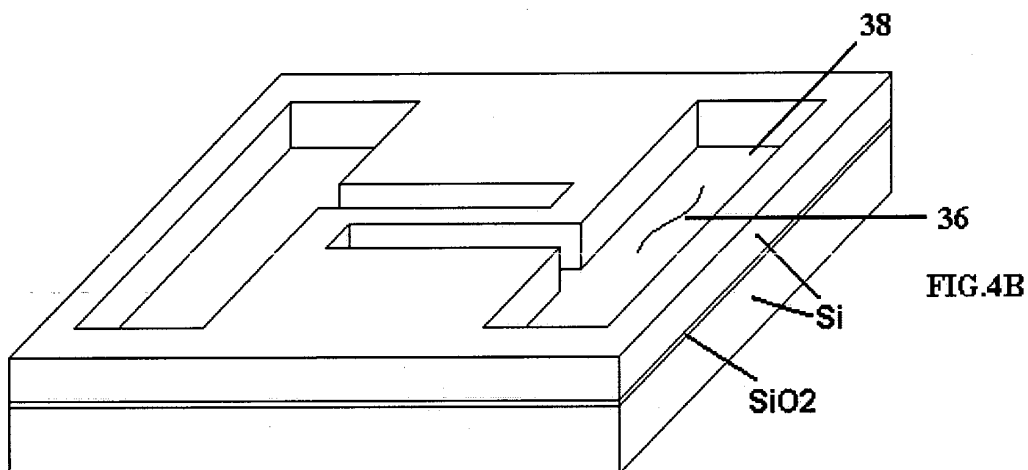
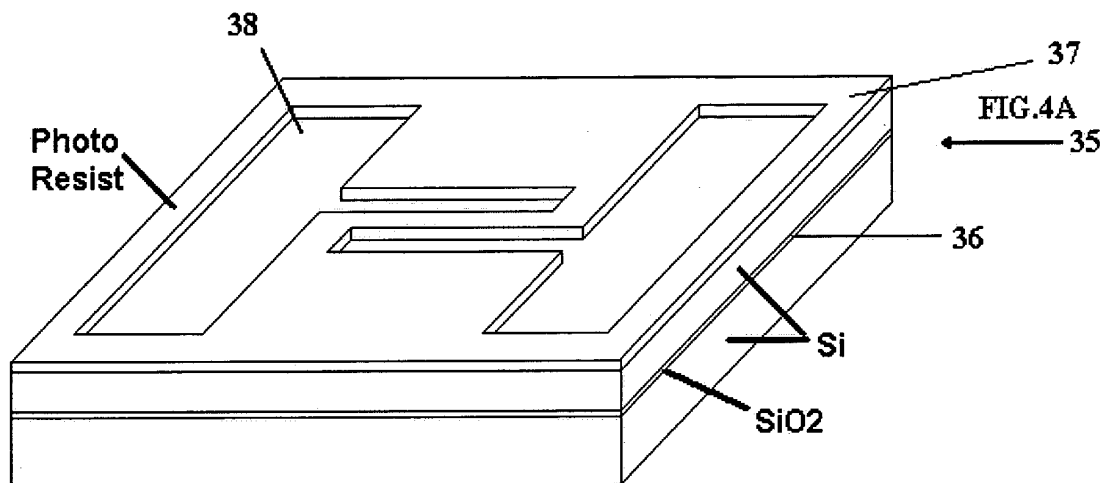


FIG. 3

Process Flow Chart Illustration



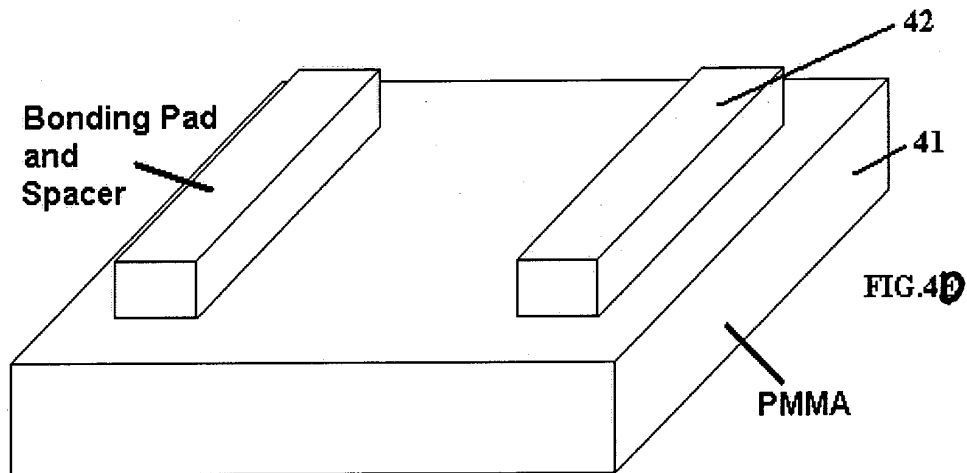


FIG.4D

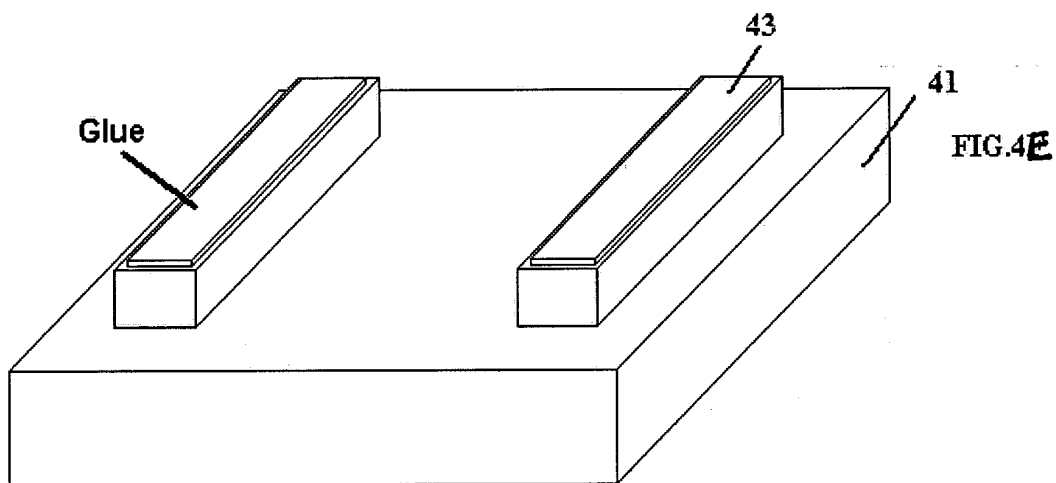
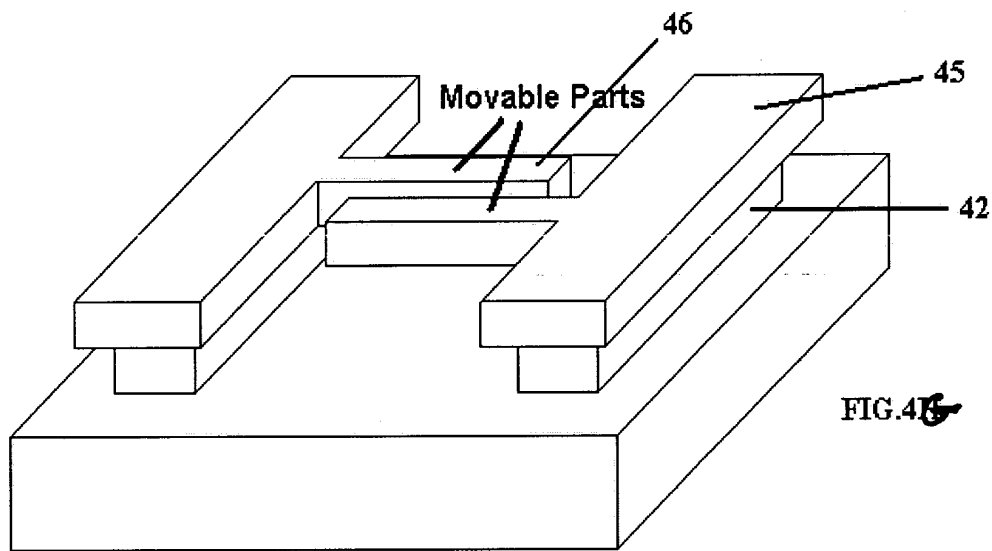
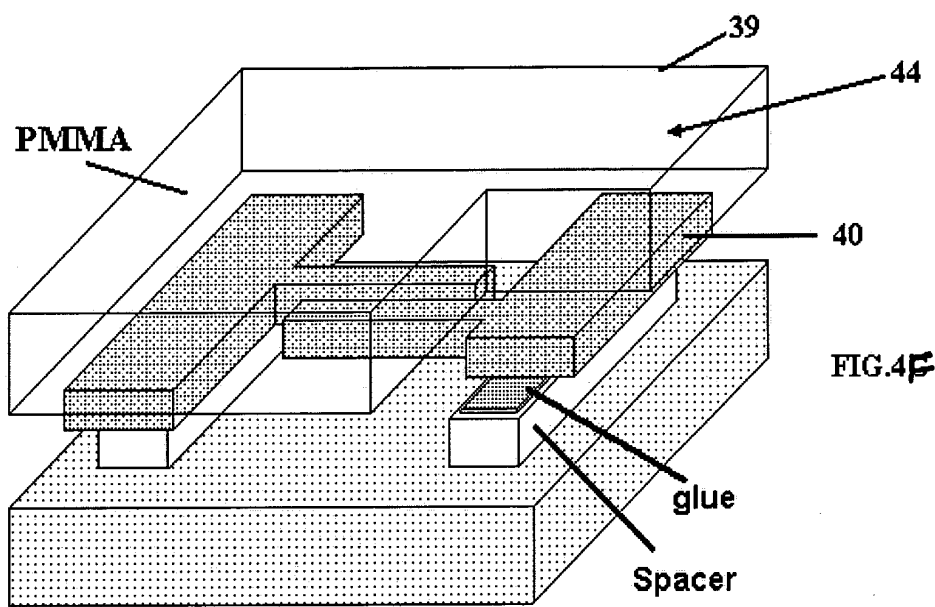
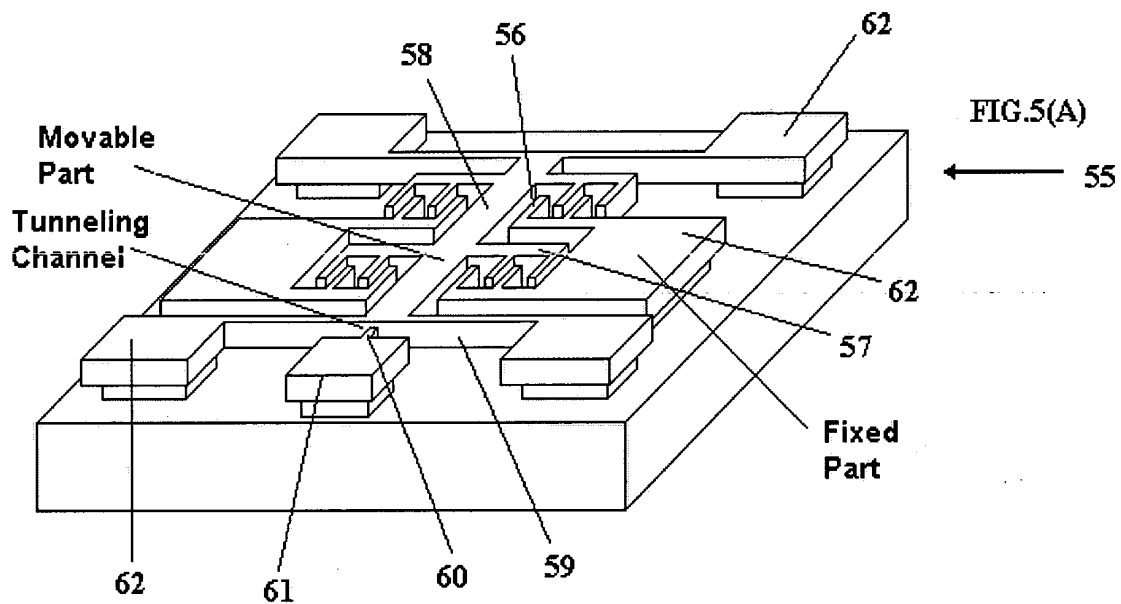
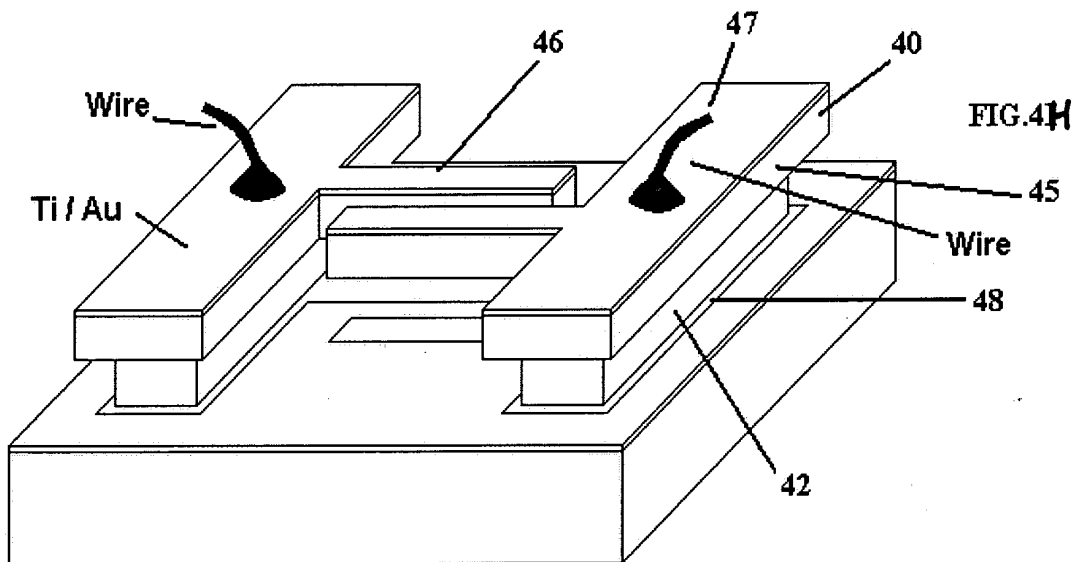


FIG.4E





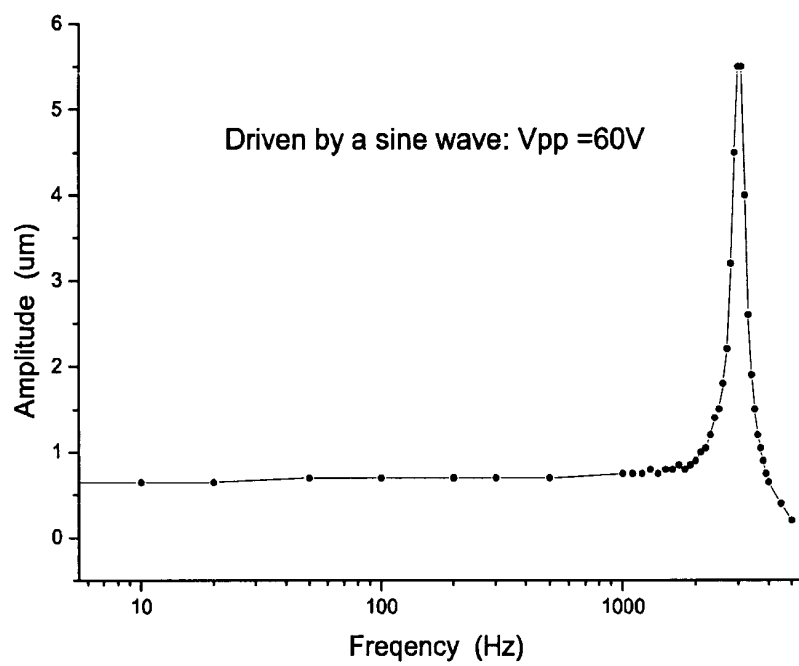
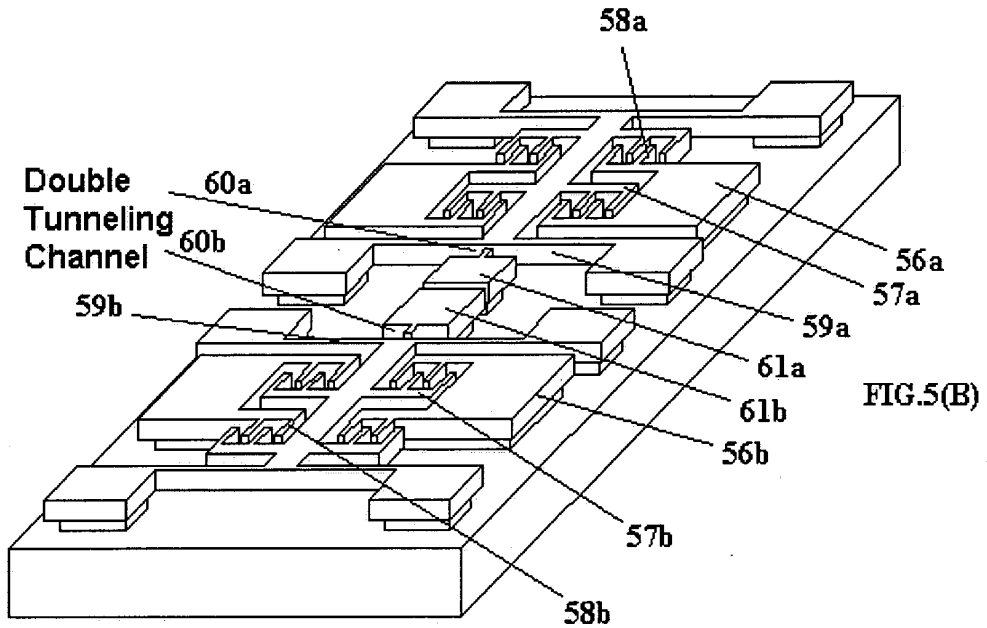


FIG.6

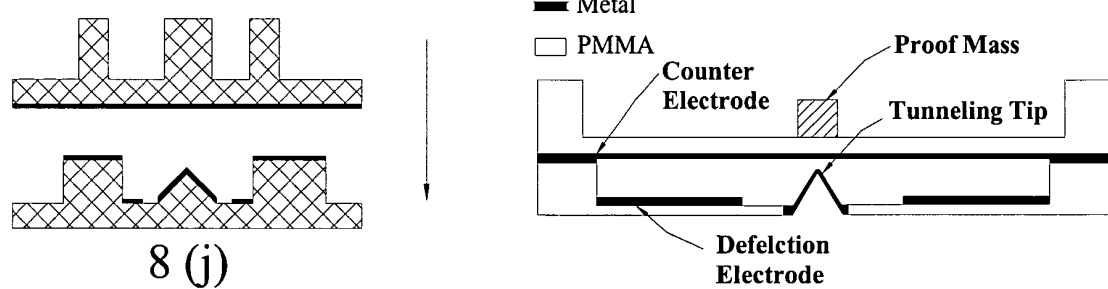
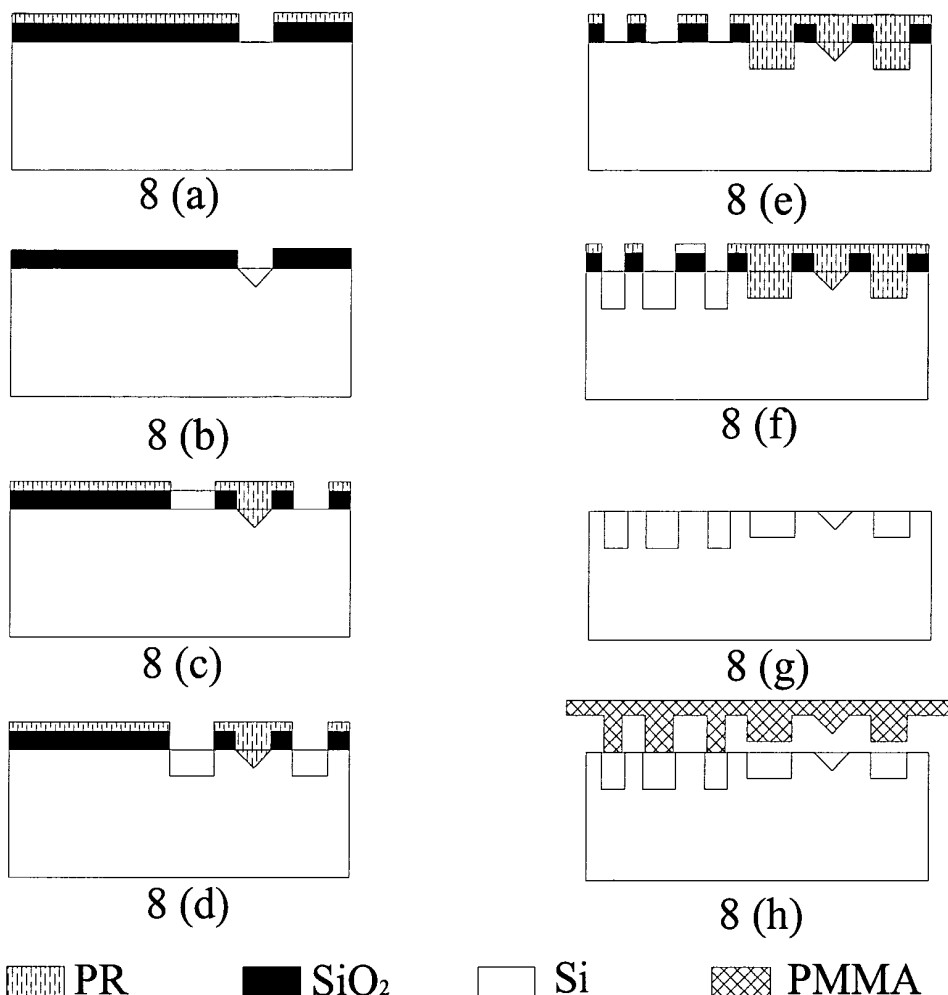


FIG. 8 (k)
Cross section of a membrane type PMMA-based tunneling sensor

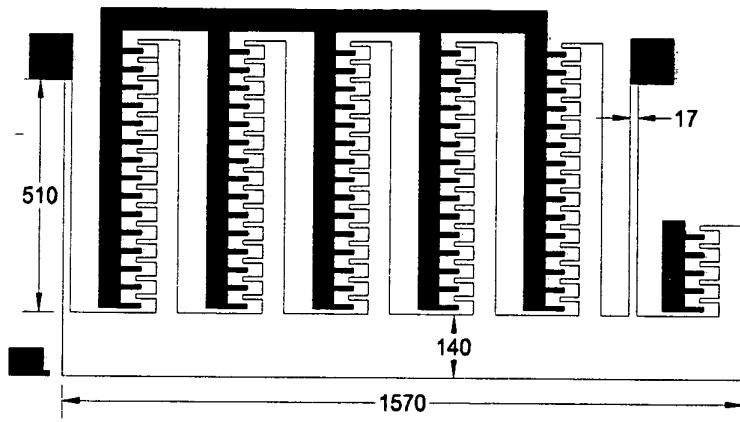


FIG 7

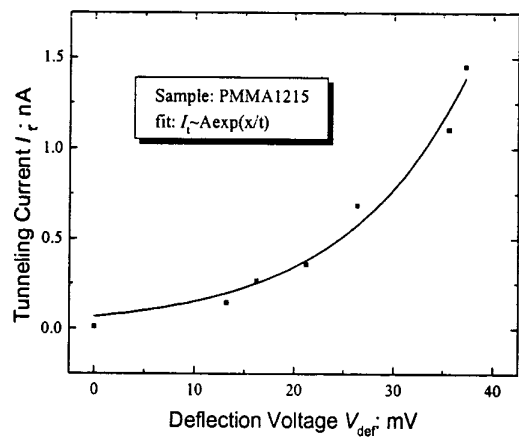


FIG. 9 The exponential relationship between
tunneling currents and applied deflection voltages